Fast-Flow EPR Spectroscopic Observation of the Isoniazid, Iproniazid, and Phenylhydrazine Hydrazyl Radicals

Impact Factor: 3.53 · DOI: 10.1021/tx0341759 · Source: PubMed

3 AUTHORS, INCLUDING:

Herbert J Sipe Jr
Hampden-Sydney College

19 PUBLICATIONS   377 CITATIONS

SEE PROFILE

Ronald P Mason
National Institute of Environmental Health S…

565 PUBLICATIONS   21,077 CITATIONS

SEE PROFILE

Fast-Flow EPR Spectroscopic Observation of the Isoniazid, Iproniazid, and Phenylhydrazine Hydrazyl Radicals

Herbert J. Sipe, Jr., Adrian R. Jaszewski, and Ronald P. Mason*

Laboratory of Pharmacology and Chemistry, National Institute of Environmental Health Sciences, National Institutes of Health, P.O. Box 12233, Research Triangle Park, North Carolina 27709

Hydrazyl radical intermediates have been suggested as important intermediates in the biochemistry of hydrazides and hydrazines. Although spin-trapping studies have intercepted those species previously, there has been no report of the direct observation of the unstable hydrazyl radicals of isoniazid and iproniazid. We have employed the fast-flow technique in electron paramagnetic resonance (EPR) spectroscopy to measure spectra for the short-lived hydrazyl radicals of a family of hydrazides, including the pharmacologically important compounds isoniazid and iproniazid, as well as for a series of phenylhydrazines. Our investigations of the phenylhydrazine radical and the related chloro-substituted analogues have allowed definitive assignments of the hyperfine coupling constants of that toxicologically important free radical. Theoretical values of hyperfine coupling constants, calculated by density functional formalism, provided a guide to assignments for the hydrazyl species and confirmed the experimentally based assignments for phenylhydrazyl radical.

Introduction

Phenylhydrazines, and particularly the parent phenylhydrazine itself, induce acute oxidative hemolytic effects (*1*). It is believed that degradation of erythrocytes in hemolytic anemia results from reaction of the hydrazine drugs with Hb[1] to form reactive hydrazyl radicals that attack and degrade erythrocyte membranes.

Isoniazid, an antituberculosis drug, and iproniazid, an antidepressant drug, in addition to their desired activities have deleterious side effects such as hemolytic anemia that may arise from their oxidation to free radical intermediates (*2*, *3*). "Activated" intermediates are formed by reaction of isoniazid with mycobacterial catalase−peroxidase enzymes and may account for the activity of isoniazid as an antitubercular drug (*4*). The nature of these activated intermediates is of continuing interest (*5−7*).

Free radical species have been observed previously via the spin-trapping technique for some of the hydrazine-based drugs and related compounds, but probably because of their reactivity and consequent short lifetimes, the initial free radical species have not been observed (*8−11*). Free radicals have been observed with fast-flow EPR for phenylhydrazine but without detailed experimental support for the EPR spectral assignments (*12*). In the present work, we have used isotopic substitution to assign the EPR hyperfine coupling constants for the phenylhydrazyl radical in detail, using a D_2O buffer system to exchange N−H to N−D and also examining a series of chloro-substituted phenylhydrazines. In addition, because of the known high reactivity of hydrazine drugs with Hb and the reported instability of the reaction intermediates, we have used the fast-flow EPR technique and a system of hydrazine drug, Hb, and H_2O_2 to successfully observe directly the isoniazid and iproniazid hydrazyl free radicals.

Materials and Methods

Chemicals and Biochemicals. Benzoic hydrazide, 2-chlorophenylhydrazine hydrochloride, 3-chlorophenylhydrazine hydrochloride, 4-chlorophenylhydrazine hydrochloride, DTPA, Hb, iproniazid, isonicotinic hydrazide (isoniazid), nicotinic hydrazide, phenylhydrazine hydrochloride, phosphoric acid-d_3 (99+ atom %D), and sodium deuterioxide 40 wt % solution in D_2O (99+ atom %D) were purchased from Sigma-Aldrich (St. Louis, MO). Reagents were used as received. The buffer for all reactions was 50 mM, pH 7.4, phosphate buffer treated with Chelex 100 resin (Bio-Rad, Hercules, CA) to remove adventitious transition metal ions and containing 1.0 mM DTPA as an additional precaution against trace metal catalysis.

EPR Experiments. Room temperature EPR spectroscopy was used to detect and identify free radical intermediates formed during reactions. Direct detection of unstable intermediates was accomplished by fast-flow EPR experiments that were performed as described previously (*13*, *14*). From a height of 1.8 m, reagents placed in solution reservoirs were allowed to flow through plastic hoses to a quartz fast-flow mixing chamber flat cell (Type WG-804, 10 mm width, Wilmad Glass Co., Buena, NJ) at rates controlled by Gilmont compact flow meters.

EPR measurements were made using either a Bruker EMX or Elexsys EPR spectrometer operating at a frequency near 9.7 GHz and a magnetic field of approximately 3480 G (Bruker Biospin, Billerica, MA). A magnetic field modulation at 100 kHz provided the usual first derivative display, and the spectrometers were fitted with the ER4122 super hi-Q microwave cavity. Spectra were recorded as computer files using Bruker's software and then analyzed, interpreted, and simulated using locally produced software (*15*). EPR figures were prepared using CorelDRAW 8 software (Corel Corporation, Ottawa, Canada) or Origin 6.0 (OriginLab Corporation, Northampton, MA).

---

* To whom correspondence should be addressed.

[1] D_2O, deuterium oxide; DFT, density functional theory; DTPA, diethylaminetriaminepentaacetic acid; EPR, electron paramagnetic resonance; H_2O_2, hydrogen peroxide; Hb, hemoglobin.
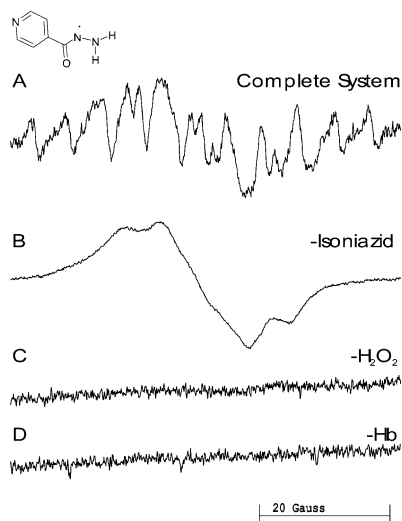
Figure 1. EPR fast-flow spectra of isoniazid hydrazyl radical produced in a system of isoniazid, H_2O_2, and Hb. The concentrations of isoniazid, H_2O_2, and Hb in the flat cell were 12.5, 12.5, and 0.092 mM. Equal volumes of isoniazid/H_2O_2 and Hb solutions in 50 mM, pH 7.4, phosphate buffer that also contained 2.0 mM DTPA were mixed milliseconds before entering the flat cell at a total flow rate of 40 mL/min. (A) Complete system with isoniazid, H_2O_2, and Hb. (B) As in panel A but no isoniazid. The intensity scale has been reduced to one-fifth that of the other spectra. (C) As in panel A but no H_2O_2. (D) As in panel A but no Hb. EPR spectra were recorded at 20 mW microwave power, 1.0 G field modulation, 60.0 G field sweep width, 41 ms time constant, 41 ms conversion time, and 36 scans of 1024 data points.

Computational Details. Quantum chemical calculations of predicted isotropic hyperfine coupling constants were performed by the Gaussian 98 program system (*16*) using Becke's one-parameter hybrid exchange functional (*17, 18*) combined with the Lee–Yang–Parr correlation functional (B1LYP) (*19*). A 6-311+G(2df,2p) extended basis set (*20, 21*) was used to refine the geometry of molecules studied, and a TZVP (triple-ζ valence polarization) basis set (*22*) with an additional *s*-type function on the heavy atoms (*23*) was used to compute the EPR parameters. Harmonic frequency analysis was performed to verify that the structures obtained were true energy minima on the molecular potential energy surfaces. For those radicals found to have multiple low energy conformers, the isotropic hyperfine coupling constants were calculated as an average of the Boltzmann population of the *N* conformers:

$$A_{iso} = [A_1 + \sum_{i=2}^{N} A_i \times \exp(-\Delta E_i/RT)]/[1 + \sum_{i=2}^{N} \exp(-\Delta E_i/RT)]$$

where A_1 is the isotropic hyperfine coupling constant of the lowest energy conformer and A_i is that of the *i*th conformer with energy E_i relative to that of the lowest conformer, R is the ideal gas constant, and T is room temperature in Kelvin.

Results

Fast-Flow EPR Experiments on Hydrazides. When solutions of benzoic acid hydrazide, nicotinic acid hydrazide, isonicotinic acid hydrazide (isoniazid), or isonicotinic acid 2-isopropyl hydrazide (iproniazid) and H_2O_2 were mixed with solutions of Hb (commercial Hb is mainly methemoglobin) under fast-flow conditions in the cavity of an EPR spectrometer, moderate to strong partially resolved EPR spectra were observed (Figure 1, isoniazid; Figure 3, iproniazid). If the experiment was repeated leaving out either the H_2O_2 or the Hb, no spectrum was observed. Flowing Hb alone against H_2O_2
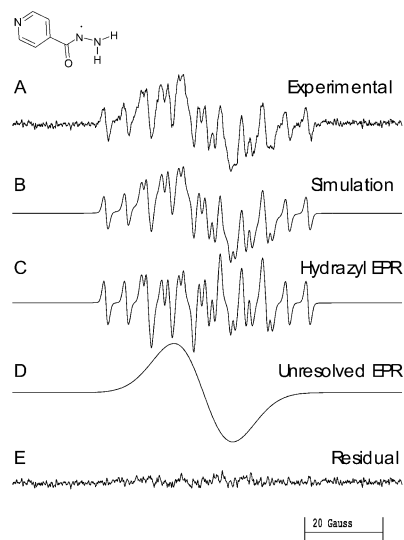

Figure 2. Analysis and simulation of isoniazid hydrazyl radical EPR spectrum. (A) Experimental spectrum: The reagent concentrations and spectrometer operating conditions were the same as in Figure 1 except that solutions were 1 mM in DTPA and 100 scans were recorded. (B) Composite simulation consisting of 14% hydrazyl radical from C plus 86% of the broad line from D. (C) Isoniazid hydrazyl radical simulation with the coupling constants given in Table 1. (D) Unresolved broad resonance with line width 7.54 G. (E) Residual plot produced when composite simulated EPR spectrum B is subtracted from experimental EPR spectrum A.
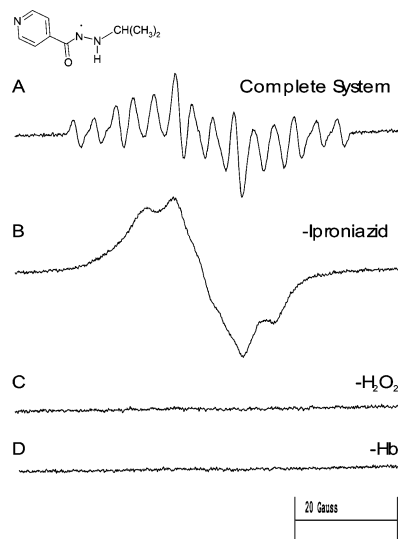

Figure 3. EPR fast-flow spectra of iproniazid hydrazyl radical produced in a system of iproniazid, H_2O_2, and Hb. The concentrations of iproniazid, H_2O_2, and Hb in the flat cell were 12.5, 12.5, and 0.092 mM. Equal volumes of isoniazid/H_2O_2 and Hb solutions in 50 mM, pH 7.4, phosphate buffer that also contained 1.0 mM DTPA were mixed milliseconds before entering the flat cell at a total flow rate of 20 mL/min. (A) Complete system with iproniazid, H_2O_2, and Hb. (B) As in panel A but no iproniazid. (C) As in panel A but no H_2O_2. (D) As in panel A but no Hb. EPR spectra were recorded at 20 mW microwave power, 1.0 G field modulation, 75.0 G field sweep width, 41 ms time constant, 41 ms conversion time, and 36 scans of 1024 data points.

in the absence of hydrazide produced a very strong unresolved broad EPR spectrum. This spectrum had been reported previously as a methemoglobin radical (*24*) and had been assigned as a partially immobilized tyrosine-derived phenoxyl radical (*25*).

The four hydrazide compounds studied here underwent facile one-electron oxidation to relatively stable hydrazyl
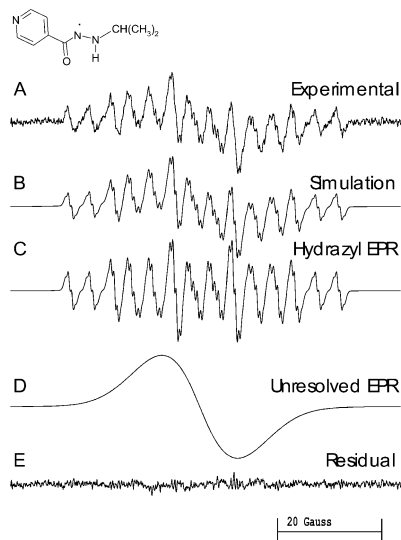
Figure 4. Analysis and simulation of iproniazid hydrazyl radical EPR spectrum. (A) Experimental spectrum: The reagent concentrations and flow conditions were the same as in Figure 3. EPR spectra were recorded at 20 mW microwave power, 0.20 G field modulation, 75.0 G field sweep width, 82 ms time constant, 82 ms conversion time, and 36 scans of 1024 points. (B) Composite simulation consisting of 17% hydrazyl radical from C plus 83% of the broad line from D. (C) Iproniazid hydrazyl radical simulation with the coupling constants given in Table 1. The simulation produced slightly better agreement with the experiment with inclusion of hyperfine coupling from three (instead of six) methyl group hydrogens. (D) Unresolved broad resonance with line width 7.66 G. (E) Residual plot produced when composite simulated EPR spectrum B is subtracted from experimental EPR spectrum A.

radicals (Figures 2 and 4). Their fast-flow EPR spectra resembled each other (cf. Figures 2A and 4A) in having total spectrum widths of about 52 G independent of the aromatic group. Examination of the outermost regions of their EPR spectra allowed direct measurement of two separate hyperfine coupling constants that appear to arise from nitrogen hyperfine interactions as indicated by the intensity patterns. By analogy with results for EPR studies of ^{15}N isotopically substituted hydrazyl radicals (26), we assigned the larger hyperfine coupling constant to the nitrogen bearing the unpaired electron; this assignment is consistent with the results of DFT calculations of the nitrogen hyperfine coupling constants for the benzoic, nicotinic, and isoniazid hydrazyl radicals. The EPR spectrum for the iproniazid hydrazyl radical had an additional small, partially resolved hyperfine splitting of ca. 0.6 G, presumably arising from hyperfine interaction of methyl group hydrogen nuclei of the isopropyl substituent, a value comparable to the 0.3 G reported for γ-hydrogen hyperfine couplings in related compounds (27).

All four hydrazide compounds gave fast-flow multiline EPR spectra with multiple hyperfine coupling constants (Table 1). Coupling constants not measured directly from the spectra were determined by computer optimization of trial spectra (15). Computer simulated fits of the experimental EPR spectra were improved by the inclusion of a contribution from a broad unresolved resonance, and the resulting residual spectrum, obtained by subtracting the experimental from the simulated spectrum, differed little from the spectrometer baseline noise signal. The EPR spectra of hydrazyl radicals from both benzoic acid hydrazide and nicotinic acid hydrazide (data not shown) closely resembled the isoniazid hydrazyl radical

Table 1. EPR Hyperfine Coupling Constants for Hydrazide Hydrazyl Radicals

X-substituent	R-substituent	a^{N}	a^{N}_{NRH}	a^{H}_{NRH}	$a^{H'}_{NRH}$
benzoic acid hydrazide	-H	9.37	5.71	11.06	10.94
nicotinic acid hydrazide	-H	9.57	5.54	11.14	11.11
isoniazid	-H	9.50 [6.7][a]	5.25 [5.9]	11.40 [-11.6]	10.85 [-11.2]
iproniazid	H$_3$C—CH—CH$_3$	4.09 [5.3]	11.38 [8.5]	11.88 [-11.8]	8.69 (1H) [5.6] 0.57 (3H) [0.27(3H), -0.10(3H)]

[a] Quantities in brackets are hyperfine coupling constants in gauss calculated by the DFT formalism. See text for details.

spectrum (Figure 2); however, the EPR spectrum of iproniazid hydrazyl radical (Figure 4) differed from that of isoniazid hydrazyl radical because of the partially resolved hyperfine structure from the isopropyl substituent of iproniazid.
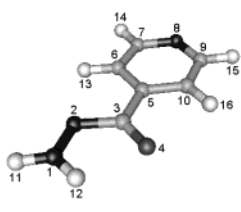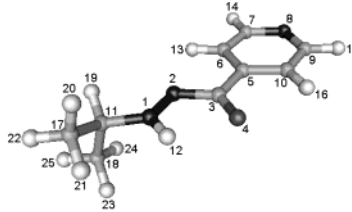
Values for the EPR hyperfine coupling constants were calculated using the DFT formalism of Gaussian 98 for hydrazyl radicals corresponding to the four hydrazide compounds studied (Table 2). In agreement with the literature reports for 1-alkyl hydrazyl radicals (26, 27), the larger nitrogen hyperfine coupling constant was calculated to arise from the divalent nitrogen atom in the isoniazid hydrazyl radical. However, DFT calculations placed the larger nitrogen hyperfine coupling constant on the trivalent nitrogen of iproniazid analogous to the literature reports for 2,2-dialkylhydrazyl radicals (26), and we have followed those results in assigning the coupling constants.

Fast-Flow EPR Experiments on Phenylhydrazines. When solutions of phenylhydrazine, 2-chlorophenylhydrazine, 3-chlorophenylhydrazine, or 4-chlorophenylhydrazine and H$_2$O$_2$ were mixed with solutions of Hb under fast-flow conditions in the cavity of an EPR spectrometer, strong well-resolved EPR spectra were observed (Figure 5). When either H$_2$O$_2$ or Hb was omitted from the system, no EPR spectrum was observed (Figure 5C,D). As was the case with the hydrazides, omission of phenylhydrazine led to a very strong, broad, unresolved EPR spectrum (Figure 5B).

EPR hyperfine coupling constants, measured from spectra recorded for fast-flow experiments, were similar for all four phenylhydrazine compounds (Table 3). On the basis of the hyperfine coupling constant assignments of Table 3, a high resolution spectrum of the phenylhydrazyl radical (Figure 6A) was simulated (Figure 6B), and the corresponding residual spectrum (Figure 6C) was essentially the same as the baseline noise.

The fast-flow EPR spectrum of the phenylhydrazyl radical has been reported previously (12), and the hyperfine coupling constant assignments were made based on the literature (12, 26). In the present study, those assignments have been verified experimentally. By comparing the total spectral width of the phenylhydrazyl

Table 2. Isotropic Hyperfine Coupling Constants (Gauss), Total Energies (Hartree), and Zero Point Vibrational Energies (kcal/mol) for Pyridylhydrazide Radicals Obtained at the UB1LYP/6-311+G(2df,2p)//UB1LYP/TZVP Level

Pyr-C(=O)-N-NH₂   Pyr-C(=O)-N-NH-CH(CH₃)₂

parameters HFCC at position	radical	
	$Pyr-C(=O)-N-NH_2$	$Pyr-C(=O)-N-NH-CH(CH_3)_2$
1	5.9	8.5
2	6.7	5.3
3	−4.9	−3.4
4	−5.4	−5.2
5	−2.5	−2.8
6	0.7	0.8
7	−0.8	−0.9
8	0.3	0.4
9	−0.7	−0.8
10	0.4	0.6
11	−11.6	−5.8
12	−11.2	−11.8
13	−0.5	−0.5
14	0.1	0.1
15	0.2	0.2
16	−0.4	−0.5
17		2.4
18		8.8
19		5.6
20		−0.3
21		−0.3
22		0.3
23		−0.5
24		−0.9
25		2.2
E_{tot}	−471.62185	−589.52369
ZPVE	75.4	128.5

Figure 5. EPR fast-flow spectra of phenylhydrazine hydrazyl radical produced in a system of phenylhydrazine, H_2O_2, and Hb. The concentrations of phenylhydrazine, H_2O_2, and Hb in the flat cell were 12.5, 12.5, and 0.18 mM. Equal volumes of phenylhydrazine/H_2O_2 and Hb solutions in 50 mM, pH 7.4, phosphate buffer that also contained 1.0 mM DTPA were mixed milliseconds before entering the flat cell at a total flow rate of 40 mL/min. (A) Complete system with phenylhydrazine, H_2O_2, and Hb. (B) As in panel A but no phenylhydrazine. (C) As in panel A but no H_2O_2. (D) As in panel A but no Hb. EPR spectra were recorded at 20 mW microwave power, 1.0 G field modulation, 60.0 G field sweep width, 41 ms time constant, 41 ms conversion time, and 36 scans of 1024 data points.

EPR spectrum successively with that of the *ortho*-, *meta*-, and *para*-chloro-substituted phenylhydrazyl EPR spectra, reasonable estimates were obtained for the hyperfine coupling constants of the protons located at those positions (Table 4). Examination of an expanded region of the low field edge of the EPR spectrum of phenylhydrazine, under somewhat overmodulated conditions, permitted the direct experimental measurement of two hyperfine coupling constants: 0.76 (1H) and 1.28 G (2H) (Table 4; data not shown). When the fast-flow EPR spectrum of the hydrazyl radical from *m*-chlorophenylhydrazine was recorded in a D₂O buffer system, the exchangeable hydrazyl protons were replaced by deuterons, and the observed spectrum width was changed correspondingly because of the smaller deuterium hyperfine coupling constants (*28*). This change was used to calculate the sum of the two hydrazyl hydrogen hyperfine coupling constants (Table 4; data not shown). Hyperfine coupling constants were also calculated using the DFT formalism for the various phenylhydrazines (Table 5).

Discussion

Previous investigators have employed methemoglobin and H_2O_2 as reagents in fast-flow EPR studies to produce the corresponding phenoxyl radicals of a wide variety of phenols (*24, 29, 30*). Smith and Maples use a phenylhy-
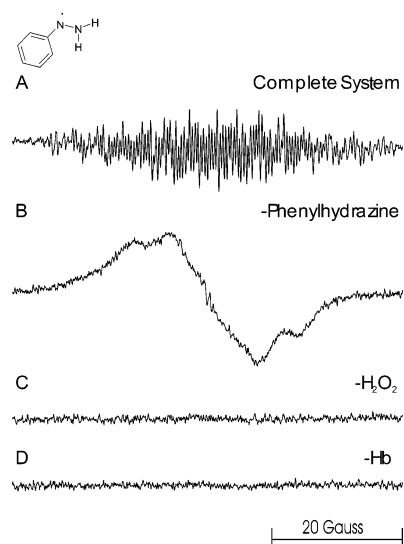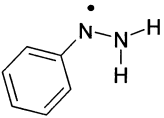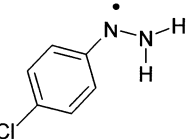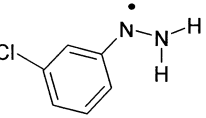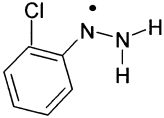
drazine/oxyhemoglobin system to observe high resolution EPR spectra of the corresponding hydrazyl radical (*12*). Several investigators previously reported EPR spin-trapping studies of nitrogen-centered free radicals from hydrazine type drugs (*8−11*) and both in vitro and in vivo observations of Hb thiyl free radical formation following exposure to hydrazines (*31−32*). These reports led us to believe that hydrazyl radicals could be observed by fast-flow EPR studies of hydrazide drugs.

When Hb alone was mixed with H_2O_2 in a flow system under our conditions, a broad, intense EPR spectrum was observed (Figures 1B, 3B, and 5B). The spectrum resembled that reported by McArthur and Davies (*25*) for a radical observed when Hb and H_2O_2 are mixed and attributed by them to a tyrosine-derived phenoxyl radical. A simulation using their EPR parameters fits the experimental spectrum moderately well (data not shown). However, whenever an oxidizable substrate such as one of the hydrazides or a phenyl hydrazine is available, the strong Hb-derived radical is not observed and the corresponding hydrazyl radical EPR spectrum is observed (see, for example, Figures 1A, isoniazid; 3A, iproniazid; and 5A, phenylhydrazine).

Solutions of benzoic acid hydrazide, nicotinic acid hydrazide, isoniazid, and iproniazid that contained H_2O_2, when mixed with solutions of Hb under fast-flow conditions, all readily formed hydrazyl radicals whose relatively strong EPR spectra were moderately well-resolved. For the three hydrazides that lack *N*-alkyl substituents, the EPR spectra were characterized by hyperfine patterns arising from two nitrogen nuclei, one about 9.5 G and the other about 5.5 G, and two hydrogen nuclei, both about 11 G. Alkyl substitution of the hydrazide group by an isopropyl group, as in iproniazid, altered this pattern by increasing one nitrogen coupling to about 11 G and

Table 3. EPR Hyperfine Coupling Constants for Phenylhydrazine Hydrazyl Radicals

Parent Compound	$a^N_{NH_2}$	a^N	$a^H_{NH_2}$	$a^{H'}_{NH_2}$	a^H_{ortho}	a^H_{meta}	a^H_{para}
phenylhydrazine	7.29 {7.14}[a] [8.7][b]	10.23 {10.11} [10.4]	3.33 {3.30} [5.3]	0.76 {0.81} [-0.9]	3.81 (2H) {3.78} [-4.7, -4.2]	1.28 (2H) {1.28} [2.0, 1.9]	4.25 {4.14} [-4.7]
4-chlorophenylhydrazine	7.26 [8.6]	10.02 [10.2]	3.59 [5.2]	0.63 [-1.1]	3.83 (2H) [-4.8, -4.2]	1.32 (2H) [2.1, 2.1]	..... [....]
3-chlorophenylhydrazine	7.40 [8.6]	9.94 [10.2]	3.69 [4.5]	0.45 [-1.6]	4.04, 3.91 [-4.5, -4.4]	1.27, ... [1.9, ...]	4.22 [-4.8]
2-chlorophenylhydrazine	7.34 [8.4]	9.67 [9.8]	4.08 [4.1]	0.51 [-1.5]	4.18, ... [-4.7, ...]	1.36 (2H) [2.1, 2.0]	4.29 [-4.8]

[a] Literature values from ref *12*. [b] Hyperfine coupling constants calculated by DFT formalism (see text).
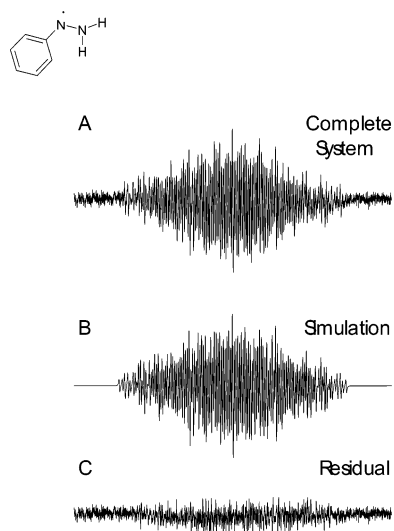

Figure 6. Analysis and simulation of phenylhydrazine hydrazyl radical EPR spectrum. (A) Experimental spectrum: The reagent concentrations were the same as in Figure 5, and the total flow rate was 25 mL/min. EPR spectra were recorded at 5 mW microwave power, 0.10 G field modulation, 75.0 G field sweep width, 82 ms time constant, 41 ms conversion time, and 114 scans of 4096 data points. (B) Phenylhydrazine hydrazyl radical simulation with the coupling constants given in Table 1. No significant improvement occurred when an unresolved broad resonance was included in the simulation. (C) Residual plot produced when simulated EPR spectrum B is subtracted from experimental EPR spectrum A.

decreasing the other to 4 G (Figure 4B). An underlying, unresolved component of the EPR spectrum was evident in the experimental spectrum, Figure 2A, and inclusion of such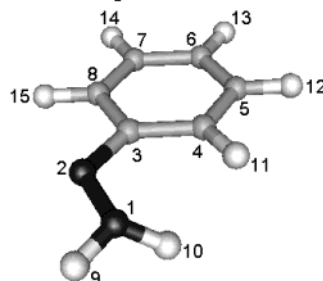 a component improved the simulation (Figure 2D). This broad resonance could arise from polymeric radical products from the hydrazyl radicals, analogous to those also seen in the spectra of tyrosyl phenoxyl radicals (*33*) or phenolphthalein phenoxyl radicals (*34*), but its is presumably from the Hb-derived radical (*25*). However, the experimental fast-flow EPR spectra were not strongly dependent on the flow rate of the experiment, which would seem to argue against polymeric radicals as the origin of the underlying resonance (data not shown). The relative flow independence is also evidence that we were likely observing radicals early in the radical generation process.

The hydrazyl radical of iproniazid, which has an isopropyl group on the terminal nitrogen of the hydrazide group, differed from the other hydrazide hydrazyl radicals in having both a larger nitrogen hyperfine interaction than the others (11.4 G > 9.5 G) and a smaller nitrogen hyperfine interaction than the others (4 G < 5.5 G). According to the DFT calculations, the larger coupling arises from the terminal nitrogen instead of the divalent nitrogen, as is the case for the unsubstituted hydrazides.

Hyperfine coupling from the hydrogen atoms of the isopropyl group was observed as a large splitting from the C−H hydrogen atom (8.7 G) and a small splitting, only partly resolved, from the C−CH₃ hydrogen nuclei (0.6 G); these parameters yielded a satisfactory simulation of the iproniazid hydrazyl radical spectrum (Figure 4B). Interestingly, the iproniazid simulation is reported for three methyl group hydrogen hyperfine interactions, not six, as expected for two methyl groups, because that produced a better overall fit between the experimental and the simulated spectrum. The DFT calculations for this radical (Table 2) are consistent with the hydrogens

Table 4. Details of Phenylhydrazine Hydrazyl Radical Hyperfine Coupling Constant Assignments

radical species	spectral width (G)	HFCC estimate
phenylhydrazyl radical	53.53	
p-chlorophenylhydrazyl	49.58	$a_{para}^{H} \cong 4.0$ G
m-chlorophenylhydrazyl	51.94	$a_{meta}^{H} \cong 1.6$ G
m-chlorophenylhydrazyl/	49.01	$a_{NH_2}^{H} + a_{NH_2}^{H'} = 4.23$ G
deuterium buffer system		
o-chlorophenylhydrazyl	49.89	$a_{ortho}^{H} \cong 3.7$ G

<div align="center">m-chlorophenylhydrazyl EPR</div>

$a^{H} = 0.45$ G (1 H)	direct measurement from edge of *m*-chlorophenylhydrazyl EPR spectrum
$a_{NH_2}^{H} + a_{NH_2}^{H'} = 4.23$ G	if $a_{NH_2}^{H'} = 0.45$, then $a_{NH_2}^{H} = 4.23-0.45 \cong 3.8$ G

<div align="center">phenylhydrazyl EPR</div>

$a^{H} = 0.76$ G (1 H)	direct measurement from edge of expanded phenylhydrazyl ESR spectrum; probably a_{NH} (see below)
$a^{H} = 1.28$ G (2 H)	direct measurement from edge of expanded phenylhydrazyl spectrum; probably a_{meta-H}
$a_{NH_2}^{H} + a_{NH_2}^{H'} = 4.23$ G	if $a_{NH_2}^{H'} = 0.76$, then $a_{NH_2}^{H} = 4.23-0.76 \cong 3.5$ G

Table 5. Isotropic Hyperfine Coupling Constants (G), Total Energies (Hartree), Zero Point Vibrational Energies (kcal/mol), and ZPV-Corrected Energy Differences (kJ/mol) for Phenylhydrazine Radicals Obtained at the UB1LYP/6-311+G(2df,2p)//UB1LYP/TZVP Level

parameters HFCC	Ph−N−NH₂	pCl−Ph−N−NH₂	mCl−Ph−N−NH₂ syn[a]	mCl−Ph−N−NH₂ anti[a]	oCl−Ph−N−NH₂ anti[a]	oCl−Ph−N−NH₂ syn[a]
1	8.7	8.6	8.5	8.6	8.4	7.0
2	10.4	10.2	10.1	10.2	9.9	9.4
3	−13.6	−13.7	−13.3	−13.4	−13.9	−14.0
4	7.8	8.0	7.7	7.7	8.0	11.0
5	−6.8	−7.0	−8.1	−6.8	−6.9	−7.5
6	7.7	9.9	7.7	7.6	7.8	8.2
7	−6.7	−7.0	−6.7	−8.0	−6.9	−7.1
8	7.2	7.3	7.2	7.3	9.7	6.7
9	−0.9	−1.1	−1.6	−1.5	−1.4	−4.6
10	5.3	5.2	4.4	4.5	4.6	−3.3
11	−4.7	−4.8	−4.7	−4.6	−4.8	0.8[b]
12	2.0	2.1	−0.3[b]	2.1	2.2	2.1
13	−4.7	0.9[b]	−4.8	−4.7	−4.8	−5.1
14	1.9	2.1	1.9	−0.3[b]	2.0	2.0
15	−4.2	−4.2	−4.2	−4.3	0.5[b]	−4.3
E_{tot}	−342.23395	−801.84918	−801.84911	−801.84877	−801.84535	−801.84228
ZPVE	76.3	70.4	70.3	70.3	70.4	70.1
ΔE^{c}			0.0	0.9	0.0	6.9

[a] Syn/anti denotes the position of the chlorine atom with regard to the N=NH₂ moiety. *[b]* Chlorine. *[c]* ZPV-corrected energy difference in respect to the conformer of the lowest energy.

of one methyl group having small (but not zero) couplings and those of the other being essentially zero. Again, the EPR spectral simulation was improved by the inclusion of a broad, unresolved component.

Phenylhydrazine is readily oxidized by the Hb/H₂O₂ system to hydrazyl radicals that have highly resolved EPR hyperfine structure, and in contrast to the hydrazide hydrazyl radicals, resolved hyperfine couplings are observed from the aromatic ring hydrogen atoms. To put the coupling constant assignments on a sound experimental basis, we recorded EPR spectra for a series of chlorophenylhydrazyl radicals. The effect of chlorine substitution, which in these cases does not significantly perturb the unpaired electron distribution in the phenyl ring, is to remove the hyperfine coupling that would correspond to that of the hydrogen atom at the position of chlorine substitution. The effect is to narrow the total spectrum width by an amount in Gauss approximately equivalent to the hyperfine coupling constant of the replaced hydrogen atom: $a^{H} \cong W_{phenylhydrazine} - W_{chlorophenylhydrazine}$. Estimates of the ortho (3.7 G), meta (1.6 G), and para (4.0 G) hyperfine coupling constants were calculated in this way from the respective widths of the spectra of the corresponding chloro-substituted phenyl-

hydrazyl radicals (see Table 4). From examination of the downfield edge of an expanded phenylhydrazyl EPR spectrum, two more hyperfine couplings can be measured directly: $a^H = 0.76$ G (1H) and $a^H = 1.28$ G (2H) (data not shown).

In a deuterium buffer system, the hydrogen atoms of the hydrazine nitrogen atoms would be expected to exchange so that the hydrazyl radical N$-$H hydrogen hyperfine interactions would be replaced by N$-$D hyperfine interactions. Assuming that the unpaired electron distribution is not affected by deuteration, each of the $a_{ND_2}^D$ hyperfine interactions can be related to the $a_{NH_2}^H$ interactions through the ratio of the magnetogyric ratios of hydrogen and deuterium. The deuterium hyperfine coupling constants are about one-sixth of the original hydrogen coupling constants. By measuring the decrease in total spectrum width of the phenylhydrazyl radical on deuteration, the sum of the two $a_{NH_2}^H$ hyperfine coupling constants can be estimated as 4.23 G. This number is too large to be either the sum of the two directly measured coupling constants ($0.76 + 1.28 = 2.04$) or twice the larger of the two directly measured coupling constants ($2 \times 1.28 = 2.56$), so it is likely that the two $a_{NH_2}^H$ couplings are different from each other and that one of them has the 0.76 value since that is the coupling constant for a unique hydrogen. With that likely assignment, the remaining $a_{NH_2}^H$ coupling constant is calculated to be about 3.5 G (Table 4).

The experimental hyperfine coupling constant values reported in Table 3 were obtained by using the NIEHS WinSim program to simulate an approximate EPR spectrum, which was optimized by comparison with the experimental EPR spectrum (Figure 6A) to produce the best simulated fit (Figure 6B). The residual pattern (Figure 6C) for the difference between the experimental and the simulated EPR spectra differed only slightly from the spectrometer noise apparent in Figure 6A. A similar approach was used to obtain experimental hyperfine coupling constants for the related phenylhydrazyl radicals reported in Table 3.

The studies reported here represent the first observations of hydrazide free radicals of the pharmaceutically important drugs isoniazid and iproniazid. Observations of these unstable free radicals were possible only because of our utilization of the fast-flow EPR technique and computer averaging of multiple spectral scans. EPR spectra for the family of hydrazide radicals were simulated using similar hyperfine coupling constants for similarly situated hydrogen and nitrogen atoms of the molecules, and the coupling constants were predicted successfully by the most modern molecular orbital calculation methods. Our investigations of the phenylhydrazyl radical and the related chloro-substituted analogues have allowed definitive assignments of the hyperfine coupling constants of that toxicologically important free radical, and the EPR results have been confirmed successfully by the molecular orbital calculations (Table 5).

In contrast to the hydrazide free radicals, the unpaired electron of phenylhydrazyl radical is significantly delocalized onto the aromatic ring. This delocalization of the spin density will lead to relative stability, which will increase the rate of radical formation in a given situation. On the other hand, the higher nitrogen atom spin densities on the hydrazide free radicals will increase their reactivity with biomolecules via such mechanisms as addition across double bonds (i.e., covalent bond formation). These differences in radical chemistry may be related to the differences in the toxicities of these compounds.

References

(1) Klaassen, C. D., Ed. (2001) *Casarett & Doull's Toxicology*, 6th ed., McGraw-Hill, New York.

(2) Halliwell, B., and Gutteridge, J. M. C. (1999) *Free Radicals in Biology and Medicine*, 3rd ed., Oxford University Press, New York.

(3) Hardman, J. G., Limbird, L. E., and Gilman, A. G., Eds. (2001) *Goodman & Gilman's The Pharmacological Basis of Therapeutics*, 10th ed., McGraw-Hill, New York.

(4) Blanchard, J. S. (1996) Molecular mechanisms of drug resistance in *Mycobacterium tuberculosis*. *Annu. Rev. Biochem. 65*, 215–239.

(5) Wengenack, N. L., and Rusnak, F. (2001) Evidence for isoniazid-dependent free radical generation catalyzed by *Mycobacterium tuberculosis* KatG and the isoniazid-resistant mutant KatG-(S315T). *Biochemistry 40*, 8990–8996.

(6) Wengenack, N. L., Hoard, H. M., and Rusnak, F. (1999) Isoniazid oxidation by *Mycobacterium tuberculosis* KatG: A role for superoxide which correlates with isoniazid susceptibility. *J. Am. Chem. Soc. 121*, 9748–9749.

(7) Bodiguel, J., Nagy, J. M., Brown, K. A., and Jamart-Gregoire, B. (2001) Oxidation of isoniazid by manganese and *Mycobacterium tuberculosis* catalase-peroxidase yields a new mechanism of activation. *J. Am. Chem. Soc. 123*, 3832–3833.

(8) Sinha, B. K., and Motten, A. G. (1982) Oxidative metabolism of hydralazine. Evidence for nitrogen centered radicals formation. *Biochem. Biophys. Res. Commun. 105*, 1044–1051.

(9) Sinha, B. K. (1983) Enzymatic activation of hydrazine derivatives. A spin trapping study. *J. Biol. Chem. 258*, 796–801.

(10) Kalyanaraman, B., and Sinha, B. K. (1985) Free radical-mediated activation of hydrazine derivatives. *Environ. Health Perspect. 64*, 179–184.

(11) Goodwin, D. C., Aust, S. D., and Grover, T. A. (1996) Free radicals produced during the oxidation of hydrazines by hypochlorous acid. *Chem. Res. Toxicol. 9*, 1333–1339.

(12) Smith, P., and Maples, K. R. (1985) EPR study of the oxidation of phenylhydrazine initiated by the titanous chloride/hydrogen peroxide reaction and by oxyhemoglobin. *J. Magn. Reson. 65*, 491–496.

(13) Josephy, P. D., Eling, T. E., and Mason, R. P. (1983) Oxidation of *p*-aminophenol catalyzed by horseradish peroxidase and prostaglandin synthase. *Mol. Pharmacol. 23*, 461–466.

(14) West, P. R., Harman, L. S., Josephy, P. D., and Mason, R. P. (1984) Acetaminophen: enzymatic formation of a transient phenoxyl free radical. *Biochem. Pharmacol. 33*, 2933–2936.

(15) Duling, D. R. (1994) Simulation of multiple isotropic spin-trap EPR spectra. *J. Magn. Reson. B 104*, 105–110.

(16) Frisch, M. J., Trucks, J. W., Schlegel, H. B., Scuseria, G. E., Robb, M. A., Cheeseman, J. R., Zakrewski, V. G., Montgomery, J. A., Jr., Stratmann, R. E., Burant, J. C., Dapprich, S., Millam, J. M., Daniels, A. D., Kudin, K. N., Strain, M. C., Farkas, O., Tomasi, J., Barone, V., Cossi, M., Cammi, R., Mennucci, B., Pomelli, C., Adamo, C., Clifford, S., Ochterski, J., Petersson, G. A., Ayala, P. Y., Cui, Q., Morokuma, K., Malick, D. K., Rabuck, A. D., Raghavachari, K., Foresman, J. B., Cioslowski, J., Ortiz, J. V., Stefanov, B. B., Liu, G., Liashenko, A., Piskorz, P., Komaromi, I., Gomperts, R., Martin, R. L., Fox, D. J., Keith, T. A., Al-Laham, M. A., Peng, C. Y., Nanayakkara, A., Gonzalez, C., Challacombe, M., Gill, P. M. W., Johnson, B., Chen, W., Wong, M. W., Andres, J. L., Head-Gordon, M., Replogle, E. S., and Pople, J. A. (1998) *Gaussian 98*, Revision A.6, Gaussian, Pittsburgh, PA.

(17) Becke, A. D. (1993) Density-functional thermochemistry. III. The role of exact exchange. *J. Chem. Phys. 98*, 5648–5652.

(18) Stephens, P. J., Devlin, F. J., Chabalowski, C. F., and Frisch, M. J. (1994) *Ab initio* calculation of vibrational absorption and

circular dichroism spectra using density functional force fields. *J. Phys. Chem. 98*, 11623−11627.

(19) Adamo, C., and Barone, V. (1997) Toward reliable adiabatic connection models free from adjustable parameters. *Chem. Phys. Lett. 274*, 242−250.

(20) Krishnan, R., Binkley, J. S., Seeger, R., and Pople, J. A. (1980) Self-consistent molecular orbital methods. XX. A basis set for correlated wave functions. *J. Chem. Phys. 72*, 650−654.

(21) Clark, T., Chandrasekhar, J., Spitznagel, G. W., and von Ragué Schleyer, P. (1983) Efficient diffuse function-augmented basis sets for anion calculations. III. The 3-21+G basis set for first-row elements, Li-F. *J. Comput. Chem. 4*, 294−301.

(22) Godbout, N., Salahub, D. R., Andzelm, J., and Wimmer, E. (1992) Optimization of Gaussian-type basis sets for local spin density functional calculations. Part I. Boron through neon, optimization technique and validation. *Can. J. Chem. 70*, 560−571.

(23) Nguyen, M. T., Creve, S., and Vanquickenborne, L. G. (1997) Efficient calculation of isotropic hyperfine constants of phosphorus radicals using density functional theory. *J. Phys. Chem. A 101*, 3174−3181.

(24) Shiga, T., and Imaizumi, K. (1975) Electron spin resonance study on peroxidase- and oxidase- reactions of horse radish peroxidase and methemoglobin. *Arch. Biochem. Biophys. 167*, 469−479.

(25) McArthur, K. M., and Davies, M. J. (1993) Detection and reactions of the globin radical in haemoglobin. *Biochim. Biophys. Acta 1202*, 173−181.

(26) Malatesta, V., Lindsay, D., Horswill, E. C., and Ingold, K. U. (1974) The EPR spectra of hydrazyl and some 1-substituted hydrazyl radicals in solution. *Can. J. Chem. 52*, 864−866.

(27) Malatesta, V., and Ingold, K. U. (1973) The electron paramagnetic resonance spectra of 1,1-dialkylhydrazyl radicals in solution. *J. Am. Chem. Soc. 95*, 6110−6113.

(28) Weil, J. A., Bolton, J. R., and Wertz, J. E. (1994) *Electron Paramagnetic Resonance: Elementary Theory and Practical Applications*, Wiley-Interscience, New York.

(29) Shiga, T., and Imaizumi, K. (1973) Generation of phenoxyl radicals by methemoglobin-hydrogen peroxide studied by electron paramagnetic resonance. *Arch. Biochem. Biophys. 154*, 540−547.

(30) Stolze, K., and Nohl, H. (1992) Methemoglobin formation from butylated hydroxyanisole and oxyhemoglobin. Comparison with butylated hydroxytoluene and *p*-hydroxyanisole. *Free Radical Res. Commun. 16*, 159−166.

(31) Maples, K. R., Jordan, S. J., and Mason, R. P. (1988) In vivo rat hemoglobin thiyl free radical formation following phenylhydrazine administration. *Mol. Pharmacol. 33*, 344−350.

(32) Maples, K. R., Jordan, S. J., and Mason, R. P. (1988) In vivo rat hemoglobin thiyl free radical formation following administration of phenylhydrazine and hydrazine-based drugs. *Drug Metab. Dispos. 16*, 799−803.

(33) Sturgeon, B. E., Sipe, H. J., Jr., Barr, D. P., Corbett, J. T., Martinez, J. G., and Mason, R. P. (1998) The fate of the oxidizing tyrosyl radical in the presence of glutathione and ascorbate. *J. Biol. Chem. 273*, 30116−30121.

(34) Sipe, H. J., Jr., Corbett, J. T., and Mason, R. P. (1997) In vitro free radical metabolism of phenolphthalein by peroxidases. *Drug. Metab. Dispos. 25*, 468−480.